

# Radical cations of non-alternant systems as probes of the Shaik–Pross VB configuration mixing model



Lennart Eberson,<sup>\*,a</sup> Remedios González-Luque,<sup>b</sup> Manuela Merchán,<sup>b</sup>  
Finn Radner,<sup>a</sup> Björn O. Roos<sup>\*,a</sup> and Sason Shaik<sup>\*,c</sup>

<sup>a</sup> Department of Chemistry, Lund University, PO Box 124, S-221 00 Lund, Sweden

<sup>b</sup> Departamento de Química Física, Universitat de València, Doctor Moliner 50, Burjassot, E-46100 València, Spain

<sup>c</sup> Institute of Chemistry and The Minerva Center of Computational Quantum Chemistry, The Hebrew University, Jerusalem, Israel

The valence bond configuration mixing (VBCM) model has been applied to predict the regioselectivity of radical cations of non-alternant systems, *viz.* dibenzofuran, dibenzothiophene, azulene, acenaphthylene and fluoranthene, toward reaction with nucleophiles. The reactivity factors of the VBCM model, the coefficients of the transfer orbital (TO) and spin densities of the lowest triplet state of each compound, have been calculated by means of high-level quantum chemical theory (CASPT2). The predictions have been compared with available experimental data. Since the expected regiochemical outcome of reactions of radical cations of this type with nucleophiles is distinctly different from that of the electrophilic reactions of the parent compounds, the approach offers a new way of testing the VBCM model. From a practical point of view, direct access to otherwise difficult to synthesize derivatives of these compounds *via* radical cation reactions should be an attractive possibility.

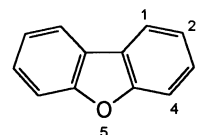
## Introduction

Understanding the reactivity of radical cations *vs.* nucleophiles still represents a major problem, despite many attempts at solving it.<sup>1</sup> The fact that radical cations sometimes obey multi-step mechanisms for simple transformations, such as nucleophilic substitution or proton abstraction, created, at one time, the impression that radical cation–nucleophile steps are intrinsically slow and must be circumvented by more complex mechanisms.<sup>2</sup>

A preliminary analysis<sup>3</sup> of the reactivity of nucleophiles (Nu:<sup>-</sup>) toward radical cations (RH<sup>•+</sup>) used the valence bond configuration mixing (VBCM) model<sup>4</sup> and ascribed the apparent slowness of the reaction to the nature of the transition state that has to involve a resonance hybrid of the reactant configuration (Nu:<sup>-</sup>/RH<sup>•+</sup>) with a doubly excited one [Nu:<sup>-</sup>/<sup>2</sup>(•RH<sup>•+</sup>)]. While this seems to provide an apparently simple rationale for the initial observations,<sup>1,2</sup> more recent experimental work has shown that quite a few radical cations react with nucleophiles *via* direct bond-forming steps, and that these steps are very fast.<sup>5</sup> Indeed, subsequent detailed VBCM analyses<sup>6</sup> demonstrated that the effect of double excitation is in fact quite small in many instances and this along with other factors will generate small barriers and fast reactions.<sup>7</sup> A recent extensive computational treatment<sup>6c</sup> establishes the potential of the VBCM model to make successful predictions of barrier height and stereochemistry of radical cation–nucleophile reactivity. The present paper further applies the VBCM model to make testable predictions of the regioselectivity of nucleophilic attack on radical cations of non-alternant aromatic systems. The reactivity parameters of the VBCM model are quantified by means of CASPT2 theory<sup>8</sup> and the predictions are compared with available experimental data. Since the area is virtually virgin, the present VBCM analysis generates also a set of *a priori* predictions, the experimental testing of which can enrich the theory upon reexamination.

It was recently shown<sup>9</sup> that the dibenzofuran radical cation (**1**<sup>•+</sup>) reacts with nucleophiles with distinctly different regioselectivity than that observed in the electrophilic attack on the

parent compound (**1**). Thus, while **1** reacts with electrophiles mainly at C-2, its radical cation **1**<sup>•+</sup> is attacked by nucleophiles



Dibenzofuran, **1** (numbering according to IUPAC rules)

predominantly at the 3- and 1-positions. This behaviour differs from most aromatic systems studied so far, where the ArH<sup>•+</sup>/nucleophile and ArH/electrophile reactions lead to similar isomer distribution.<sup>10</sup> Since **1** is a non-alternant system, the pairing theorem<sup>11</sup> does not apply and therefore the different reactivity of **1** and **1**<sup>•+</sup> must reflect the involvement of different orbitals. The VBCM model predicts that the regioselectivity of nucleophilic attack on a radical cation should be determined by a combination of the LUMO coefficients of the radical cation and the triplet spin density in the neutral parent, and theoretical calculations of these quantities demonstrated this prediction to be correct.<sup>9a</sup>

Thus it appears that the reactions of radical cations of non-alternant systems might provide novel tests of the VBCM model, which avoid the difficulty of defining 'fast' and 'slow' radical cation–nucleophile steps. In what follows, we present an application of the VBCM model which involves theoretical calculations<sup>8</sup> of relevant reactivity indices by high-level *ab initio* theory for a set of non-alternant systems: dibenzofuran (**1**), dibenzothiophene (**2**), azulene (**3**), acenaphthylene (**4**) and fluoranthene (**5**). These systems were chosen on the basis of the feasibility of possible future detailed experimental testing of the predicted regiochemistry. Presently, the predictions about radical cation–nucleophile reactivities of these systems can only be calibrated against the rather limited amount of experimental results available; it is our hope that experimentalists will find the results interesting enough to warrant further studies of these demanding problems.

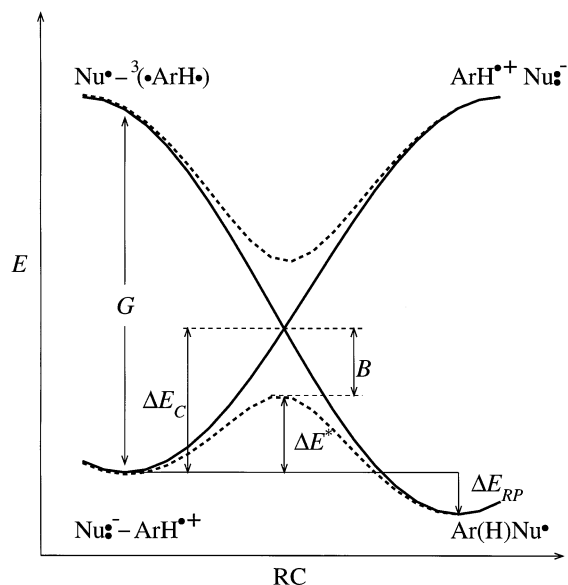


**Fig. 1** A curve crossing diagram for the nucleophilic addition process,  $\text{Nu:}^- + \text{ArH}^{\bullet+} \longrightarrow (\cdot\text{ArHNu})$ . The reactant state refers to the geometry of the encounter complex. Electrons are shown by heavy dots.

## Results and discussion

### Application of the VBCM model to the formation of regioisomers from radical cation-nucleophile reactions

The basic features of the VBCM treatment are indicated in Fig. 1, which shows the curve crossing situation for a reaction of nucleophile  $\text{Nu:}^-$  with an arene radical cation ( $\text{ArH}^{\bullet+}$ ).<sup>12</sup> The gap,  $G$ , is the difference between the energy of the reactant state ( $\text{Nu:}^-/\text{ArH}^{\bullet+}$ ) and the excited product configuration [ $\text{Nu}^\bullet/{}^3(\text{ArH})$ ] at the geometry of the reactant.  $B$  is the avoided crossing quantity or simply the resonance energy of the transition state. Finally,  $\Delta E_C$  is the height of the crossing point above the reactant cluster (encounter complex). The height of the central barrier,  $\Delta E^*$ , is given most simply by eqn. (1).<sup>13</sup>

$$\Delta E^* = \Delta E_C - B; \Delta E_C/G = f \quad (1)$$

While it is apparent from Fig. 1 that  $\Delta E_C$  is a fraction of the gap  $G$ , there exist several ways to express this fundamental relationship explicitly by approximations of the curve functions.<sup>13</sup> Eqn. (2) is the simplest such expression which captures

$$\Delta E_C \approx f_0 G + (0.5 - f_0) \Delta E_{\text{RP}} \quad (2)$$

the qualitative essence of the  $\Delta E_C/G$  relation in eqn. (1) as well as leading to satisfactory quantitative estimates of the height of the crossing point.<sup>6c</sup>

$\Delta E_C$  is seen to depend on the reaction thermodynamic quantity  $\Delta E_{\text{RP}}$  and on the 'intrinsic' quantity  $f_0 G$ . As the reaction becomes more exothermic ( $\Delta E_{\text{RP}}$  more negative) the crossing point becomes lower and *vice versa* for an endothermic process. For a thermoneutral case the crossing point is dominated by the intrinsic property  $f_0 G$  where  $f_0$  depends on the steepness of the curves. Using eqn. (2) the barrier is given by eqn. (3).

$$\Delta E^* = f_0 G + (0.5 - f_0) \Delta E_{\text{RP}} - B \quad (3)$$

We now apply the model, using eqn. (3) as an aid, to the regiochemical problem. Since the regioisomers are nascent from the same reactant state, the  $G$  factor is common to all regiochemical pathways, and uncertainty in  $G$  due to complexation is not crucial for the problem at hand. Furthermore, in most cases,<sup>14</sup> the relative stability of regioisomers is not much different from unity. Therefore, the regioselectivity should depend primarily on the factors  $f_0$  and  $B$ , much as discussed previously for the corresponding problem in radical addition to olefins.<sup>14</sup>

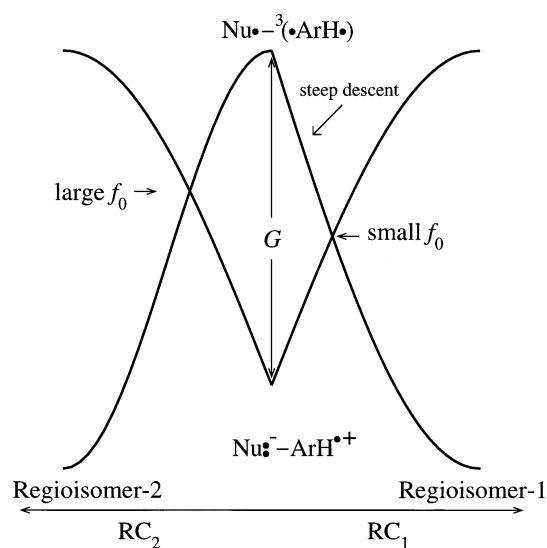
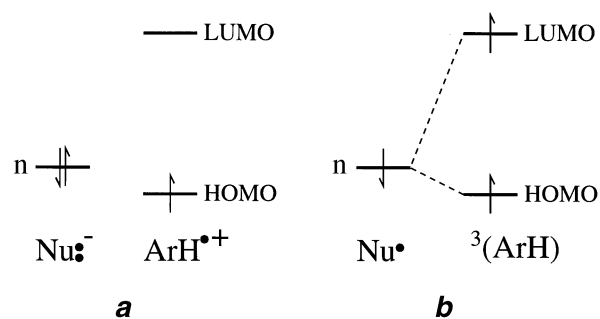


**Fig. 2** Illustration of the effect of the steepness of descent of the  $\text{Nu}^\bullet/{}^3(\text{ArH})$  state on the height of the crossing point  $f_0 G$

Fig. 2 shows the curve crossing situations (without avoided crossing) for formation of two regioisomers designated as 1 and 2. The two diagrams have common reactant and excited states, and hence also a common onset in the middle of Fig. 2. The diagrams illustrate the effect of  $f_0$  [eqn. (2)] on the height of the crossing points for the two pathways. It is seen that a steeper descent of the excited state, as drawn arbitrarily for regioisomer 1, produces a lower crossing point [smaller  $f_0$  in eqn. (2)]. The descent of the excited state is due to the bond coupling of the odd electron in  $\text{Nu}^\bullet$  with the odd electrons of  ${}^3(\text{ArH})$ ,<sup>6c</sup> which finally becomes the ground product state, ( $\text{ArHNu}^\bullet$ ). We may therefore state the first regioselectivity rule:

*The regiochemical pathway with the smaller  $f_0$  will be associated with attack on the site of highest spin density in the triplet  ${}^3(\text{ArH})$  species.*

The second regioselectivity factor is  $B$ , the resonance energy of the transition state (Fig. 1) due to the mixing of the two configurations ( $\text{Nu:}^-/\text{ArH}^{\bullet+}$ ) and [ $\text{Nu}^\bullet/{}^3(\text{ArH})$ ].<sup>6c</sup> Taking the two generic configurations<sup>15</sup> **a** and **b** in Scheme 1, the  $\text{ArH}$



**Scheme 1**

would be represented by the two orbitals labelled as HOMO and LUMO<sup>15</sup> and the nucleophile by the orbital  $n$ . The resonance energy  $B$  between the configurations is proportional to the overlap between the orbital of the nucleophile ( $n$ ) and the LUMO of the radical cation. The second regiochemical rule may therefore be stated as follows:

*The regiochemical pathway with the larger resonance energy  $B$  will be associated with nucleophilic attack at the position with the highest coefficient of the LUMO of the radical cation.*

We note that the orbital labelled as LUMO is singly occupied in the triplet moiety (**b**, Scheme 1), and in fact this is the orbital which accepts the electron which is transferred from the nucleophile. We shall refer to this orbital as the transfer orbital (TO)

**Table 1** CASPT2 relative energies in eV for the different electronic states of some non-alternant systems and their radical cations

System	State	CASPT2	Experimental value(s)	Previous <i>ab initio</i> calculation(s)
<b>1</b>	<sup>3</sup> B <sub>2</sub>	3.46	3.04; <sup>a</sup> 2.97; <sup>b</sup> 3.03 <sup>c</sup>	3.61 <sup>d</sup>
	<sup>3</sup> A <sub>1</sub>	3.94		4.15 <sup>d</sup>
<b>1<sup>•+</sup></b>	<sup>2</sup> A <sub>2</sub>	8.11	8.40; <sup>e</sup> 8.3 <sup>f</sup>	8.15 <sup>d</sup>
	<sup>2</sup> B <sub>1</sub>	8.07	8.40; <sup>e</sup> 8.1 <sup>f</sup>	8.71, 8.22, 8.63, 6.42 <sup>g</sup> , 8.18 <sup>d</sup> , 8.70, 8.68, 9.06, 6.56 <sup>g</sup>
<b>2</b>	<sup>3</sup> B <sub>2</sub>	3.29	3.01; <sup>h</sup> 2.95; <sup>b</sup> 3.02 <sup>i</sup>	
	<sup>3</sup> A <sub>1</sub>	3.84		
<b>2<sup>•+</sup></b>	<sup>2</sup> A <sub>2</sub>	7.96	8.36; <sup>j</sup> 8.34 <sup>f</sup>	8.27, 8.63, 6.29 <sup>g</sup>
	<sup>2</sup> B <sub>1</sub>	7.46	8.01; <sup>j</sup> 7.93 <sup>f</sup>	8.79, 9.02, 5.94 <sup>g</sup>
<b>3</b>	<sup>3</sup> B <sub>2</sub>	2.11	1.69; <sup>k</sup> 1.72 <sup>l</sup>	
	<sup>3</sup> A <sub>1</sub>	2.25		
<b>3<sup>•+</sup></b>	<sup>2</sup> A <sub>2</sub>	7.12	7.43; <sup>m</sup> 7.44 <sup>n</sup>	
	<sup>2</sup> B <sub>1</sub>	8.36	8.50; <sup>o</sup> 8.48; <sup>p</sup> 8.51 <sup>n</sup>	
<b>4</b>	<sup>3</sup> B <sub>2</sub>	2.35	2.38; <sup>q</sup> 1.99–2.04 <sup>r</sup>	
	<sup>3</sup> A <sub>1</sub>	2.75		
<b>4<sup>•+</sup></b>	<sup>2</sup> A <sub>2</sub>	8.18	8.39 <sup>s</sup>	
	<sup>2</sup> B <sub>1</sub>	7.77	8.22; <sup>s</sup> 8.02 <sup>t</sup>	
<b>5</b>	<sup>3</sup> B <sub>2</sub>	2.87		
	<sup>3</sup> A <sub>1</sub>	2.59	2.29; <sup>u</sup> 2.30; <sup>v</sup> 2.24; <sup>w</sup> 2.06 <sup>x</sup>	
<b>5<sup>•+</sup></b>	<sup>2</sup> A <sub>2</sub>	7.58	7.95; <sup>y</sup> 7.80 <sup>z</sup>	
	<sup>2</sup> B <sub>1</sub>	7.80	8.1 <sup>y</sup>	

<sup>a</sup> Ref. 50. <sup>b</sup> Ref. 51. <sup>c</sup> Ref. 52. <sup>d</sup> Ref. 9a. <sup>e</sup> Ref. 49. <sup>f</sup> Ref. 53. <sup>g</sup> Ref. 54. <sup>h</sup> Ref. 51a. <sup>i</sup> Ref. 55. <sup>j</sup> Ref. 56. <sup>k</sup> Ref. 57. <sup>l</sup> Ref. 58. <sup>m</sup> Ref. 59. <sup>n</sup> Ref. 60. <sup>o</sup> Ref. 59a,b. <sup>p</sup> Ref. 59d. <sup>q</sup> Ref. 61. <sup>r</sup> Ref. 62. <sup>s</sup> Ref. 59c. <sup>t</sup> Ref. 59b. <sup>u</sup> Ref. 63. <sup>v</sup> Ref. 64. <sup>w</sup> Ref. 61. <sup>x</sup> Ref. 65. <sup>y</sup> Ref. 59c. <sup>z</sup> Ref. 59b.

rather than the LUMO in order to make the necessary connection to the CASSCF results (see Methods).

Summarizing, for cases where the isomer stability is not extremely different,<sup>14c</sup> the isomer distribution from the reaction between Nu:• and ArH<sup>•+</sup> should be governed by a combination of two indices, the spin density distribution and the TO coefficients of the lowest triplet state of ArH. If both are significant at a specific site, there should be a high probability of attack; if either or both indices are small, the probability of attack at the corresponding site should be low.

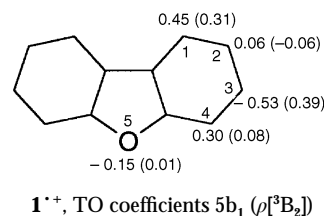
This is a simple and straightforward model of regioselectivity which allows us to make predictions and to test them. As any simple model, this also has inherent assumptions and caveats which are required for making predictions in cases of complex molecular systems. These limitations are outlined in the Methods section which shows how the generic predictions nevertheless emerge from the complex problem.

### Dibenzofuran: a test case

Dibenzofuran was chosen as a test case, mainly because of the relative abundance of experimental data on its radical cation mediated reactions. Accurate theoretical calculations of relative energies of the relevant electronic states of dibenzofuran (**1**) and its radical cation (**1<sup>•+</sup>**) are given in Table 1 (for details of the calculations, see below). The two lowest radical cation states are nearly degenerate, the <sup>2</sup>B<sub>1</sub> state being only 0.12 eV below the <sup>2</sup>A<sub>2</sub> state. However, experimentally <sup>2</sup>A<sub>2</sub> is found to be the ground state (see below). Using this ground state as configuration *a* and <sup>3</sup>B<sub>2</sub> as the triplet moiety in configuration *b* (Scheme 1) we obtain the indices shown below for **1<sup>•+</sup>**, taken from Table 2.

Clearly the attack of a nucleophile upon **1<sup>•+</sup>** would be predicted to occur in the order of positions 3 ≈ 1 > 4 > 2. This prediction persists even if the radical cation is considered to be the degenerate mixture of states, <sup>2</sup>B<sub>1</sub> ± <sup>2</sup>A<sub>2</sub> (see Methods section).

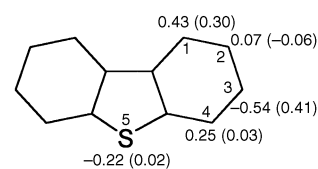
Which are the experimental results? Table 3 lists results from the determination of isomer distributions of reactions of **1<sup>•+</sup>** with a few nucleophiles. The **1<sup>•+</sup>**-nucleophile reactions differ somewhat with respect to isomer distribution depending on the



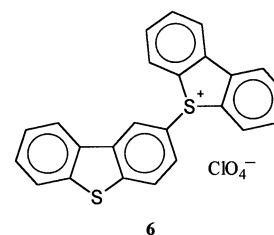
nature of the nucleophile, but the main feature is still a preponderance for attack at the 3- and 1-positions, contrary to the situation in electrophilic reactions of **1** where the main centres of attack are the 2- (predominantly) and 4-positions. The variations within the set of **1<sup>•+</sup>**-nucleophile reactions are not easily analysed for several reasons: the 1-position is subject to steric hindrance from the 9-hydrogen to an unknown extent (*cf.* protodesilylation of 1-Me<sub>3</sub>Si-**1** vs. protodetrithiation of 1,9-di[<sup>2</sup>H<sub>2</sub>]-**1**)<sup>16</sup> and it may also be that a switch from a hard nucleophile (acetate ion) to a softer one (trinitromethanide ion) causes the thermodynamic stability of Ar'(H)Nu to become important.

### Dibenzothiophene (**2**)

The electronic properties of **2** and **2<sup>•+</sup>** are similar to those of **1** and **1<sup>•+</sup>**. The lowest triplet state of **2** is of <sup>3</sup>B<sub>2</sub> type whereas the <sup>2</sup>B<sub>1</sub> state is the lowest radical cation state. The relevant reactivity indices (Table 2) are shown below, with ρ[<sup>3</sup>B<sub>2</sub>] given within parentheses. Thus, we predict a similar outcome in **2<sup>•+</sup>**-nucleophile reactions as in those of **1<sup>•+</sup>**, with positions 3 and 1, in that order, more reactive than the 2- and 4-positions.



In electrophilic substitution, **2** behaves analogously to dibenzofuran **1** by being attacked mainly in the 2-position with the 4-position coming second.<sup>17</sup> Relevant experimental data for reactions between **2<sup>•+</sup>** and nucleophiles are practically non-existent. Examples of the electron transfer mediated substitution of **2** are limited to studies of anodic dimerization, which was claimed to occur at the 2-position, attack occurring *via* the sulfur atom of the second dibenzothiophene moiety to give eventually **6**. However, it is not known whether this reaction is



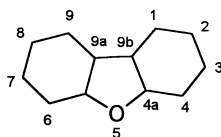
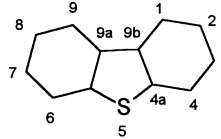
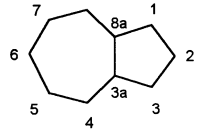
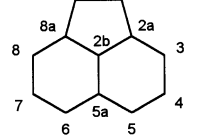
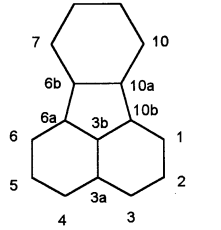
of radical cation-nucleophile (**2** attacking **2<sup>•+</sup>**) or radical cation-radical cation (coupling between two **2<sup>•+</sup>**) and the assignment of **6** as being 5,2'-connected was not proved.<sup>18</sup>

### Azulene (**3**)

Similar treatment of the azulene data produces the following reactivity maps for **3<sup>•+</sup>**-nucleophile reactions. For reaction between **3<sup>•+</sup>** and nucleophiles, the VBCM model predicts attack at the 4(8)- and 6-positions while position 2 should come third.

Electrophilic substitution in azulene occurs with very high selectivity at the 1(3)-position, no other isomer being formed.<sup>19</sup> Examples of possibly radical cation mediated reactions of **3** are limited to a rather unusual type of oxidative substitution, in

**Table 2** Transfer orbital (TO) coefficients and spin densities of radical cation and triplet states of 1–5. The numbering system follows IUPAC rules

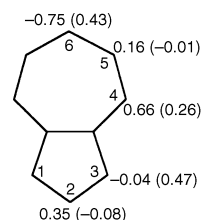
System	State	Index										
Dibenzofuran (1) 	$^2A_2$	Atom No.	1	2	3	4	5	4a	9b			
		Spin density	0.09	-0.05	0.29	-0.09	0.00	0.17	0.10			
	$^2B_1$	Spin density	0.07	0.21	-0.10	0.19	0.09	0.08	0.01			
		TO coeff.	0.45	0.06	-0.53	0.30	-0.15	0.26	-0.41			
	$^3B_2$	Spin density	0.31	-0.06	0.39	0.08	0.01	0.12	0.16			
		Spin density	0.31	0.16	0.05	0.33	0.02	0.12	0.02			
Dibenzothiophene (2) 	$^2A_2$	Atom No.	1	2	3	4	5	4a	9b			
		Spin density	0.13	-0.08	0.29	-0.08	0.01	0.15	0.08			
	$^2B_1$	Spin density	0.01	0.17	-0.09	0.17	0.35	0.03	0.05			
		TO coeff.	0.43	0.07	-0.54	0.25	-0.22	0.31	-0.42			
	$^3B_2$	Spin density	0.30	-0.06	0.41	0.03	0.02	0.17	0.15			
		Spin density	0.31	0.15	0.03	0.34	0.04	0.01	0.13			
Azulene (3) 	$^2A_2$	Atom No.	2	3	4	5	6	3a				
		Spin density	-0.19	0.44	-0.07	0.19	-0.07	.07				
	$^3B_2$	TO coeff.	0.35	-0.04	0.66	0.16	-0.75	-0.47				
		Spin density	-0.08	0.47	0.26	-0.01	0.43	0.11				
$^3A_1$	Spin density	0.00	0.39	0.11	0.38	0.02	0.11					
	Spin density											
Acenaphthylene (4) 	$^2B_1$	Atom No.	2	3	4	5	2a	2b	5a			
		Spin density	0.33	0.03	-0.02	0.09	-0.02	0.21	-0.02			
	$^3B_2$	TO coeff.	0.69	-0.56	-0.08	0.49	0.22	0.00	0.00			
		Spin density	0.58	0.33	-0.13	0.31	-0.13	0.16	-0.06			
$^3A_1$	Spin density	0.07	0.14	0.07	0.41	0.36	-0.05	-0.07				
	Spin density											
Fluoranthene (5) 	$^2A_2$	Atom No.	1	2	3	9	10	3a	3b	10a	10b	
		Spin density	0.05	0.10	0.24	0.06	0.11	-0.02	-0.16	-0.09	0.12	
	$^3B_2$	TO coeff.	-0.31	-0.41	0.63	0.17	-0.20	0.00	0.00	0.27	0.64	
		Spin density	0.02	0.29	-0.01	0.15	0.05	-0.01	0.05	0.38	0.11	
	$^3A_1$	Spin density	0.09	0.11	0.35	0.05	0.04	-0.13	-0.07	0.01	0.44	
		Spin density										

**Table 3** Isomer distributions from various reactions between dibenzofuran radical cation  $1^{+\cdot}$  and nucleophiles.

Reaction of $1^{+\cdot}$ with	Isomer distribution (%)				Ref.
	1-	2-	3-	4-	
CN <sup>-</sup> in MeOH (anodic)	8	17	71	4	9b
CN <sup>-</sup> in MeOH ( <i>hν</i> )	9	27	64	<0.5	9b
AcO <sup>-</sup> in HOAc (anodic)	32	3	62	3	9c
AcO <sup>-</sup> in HOAc [12-tungstocobaltate(III)]	42	1	55	2	9c
AcO <sup>-</sup> in HOAc [Ce <sup>IV</sup> (NO <sub>3</sub> ) <sub>6</sub> <sup>2-</sup> ]	32	2	64	2	9c
AcO <sup>-</sup> in HOAc (Ag <sup>II</sup> -S <sub>2</sub> O <sub>8</sub> <sup>2-</sup> )	29	1	70	9c	9c
(NO <sub>2</sub> ) <sub>2</sub> C <sup>-</sup> in CH <sub>2</sub> Cl <sub>2</sub> [ <i>hν</i> with C(NO <sub>2</sub> ) <sub>4</sub> ]	62		38		66
(NO <sub>2</sub> ) <sub>2</sub> C <sup>-</sup> in CH <sub>3</sub> CN [ <i>hν</i> with C(NO <sub>2</sub> ) <sub>4</sub> ]	51		49		66
F <sup>-</sup> in CF <sub>3</sub> COOH [F-TEDA] <sup>a</sup>	22	39	39		67

<sup>a</sup> F-TEDA is 1-chloromethyl-4-fluoro-1,4-diazoniabicyclo[2.2.2]octane bis(tetrafluoroborate) which is assumed to react *via* a blend of a polar and radical cation mediated mechanism.

which azulene was allowed to react with copper(II) nitrite in pyridine, suggested to occur by reaction between  $3^{+\cdot}$  and nitrite ion.<sup>20</sup> This reaction provided a 2 : 1 mixture of 1- and 2-nitroazulene, formation of the latter being a highly unusual regiochemistry of azulene and to our knowledge the only instance in which substitution at an azulene position other than 1(3)- has been found. Similar studies involving other nucleophiles (thiolates, sulfite ion, bromide ion) led to 1-substituted compounds

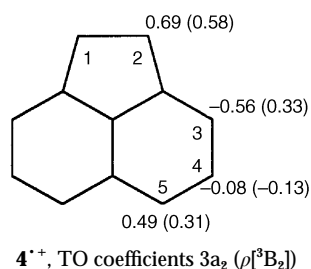
 $3^{+\cdot}$ , TO coefficients  $4b_1$  ( $\rho[{}^3B_2]$ )

only.<sup>21</sup> It is not clear whether these cases are relevant for the discussion here. The experimental verification of the regioselectivity of  $3^{+\cdot}$  toward nucleophiles is likely to involve a number of difficult problems due to its high reactivity, but also carries synthetic rewards in terms of direct access to 4(8)- and/or 6-substituted azulenes.

#### Acenaphthylene (4)

The same treatment of the acenaphthylene data produces the following reactivity maps for  $4^{+\cdot}$ -nucleophile reactions. For reaction between  $4^{+\cdot}$  and nucleophiles it is predicted that the order of regioselectivity would be attack at the C-1(2)- > C-3(8)- ~ C-5(6)-positions.

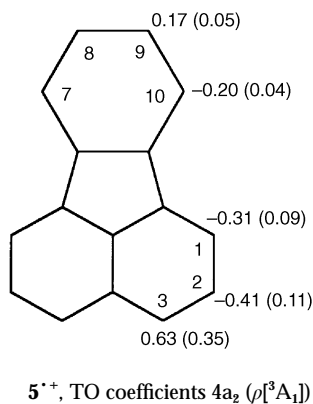
The known electrophilic chemistry of acenaphthylene classi-



fies it as a reactive olefin, attack occurring mainly at the 1(2)-position.<sup>22</sup> These positions also give the thermodynamically most stable isomers. Nevertheless the VBCM model suggests finite regioselectivity at C-3 and C-5. Thus, the prediction about the differing regiochemistry of  $4^{+\bullet}$ -nucleophile reactions might be a crucial test of the VBCM model. Few studies of relevance to this problem have been published. The reaction between **4** and chlorine dioxide in water has been suggested to occur by formation of  $4^{+\bullet}$ , followed by its reaction with water to give the 1,2-dihydro-1,2-diol and corresponding chlorohydrin.<sup>23</sup> Lead tetraacetate induced bismethoxylation and bisacetoxylation of **4**, which might be of electrophilic nature, occur across the 1,2-positions,<sup>24</sup> and the ammonium hexanitratocerate(IV) oxidation of **4** in acetonitrile in the presence of azide ion gave the *trans*-1-azido-2-nitrato adduct.<sup>25</sup> The latter reaction was formulated as proceeding *via* initial attack by azide radical, but a radical cation-azide ion mechanism is also possible in view of later studies on  $Ce^{IV}$  oxidation.<sup>26</sup> The mechanistic ambiguities of these reactions call for further studies of reactions of a mechanistically well-defined nature.

#### Fluoranthene (5)

Finally, the same treatment of the fluoranthene data produces the following reactivity map for  $5^{+\bullet}$ -nucleophile reactions. Predictions for  $5^{+\bullet}$ -nucleophile reactions are that the 3(4)-positions



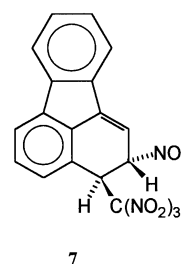
should be favoured over the 1(6)- and 2(5)-positions and that little attack should occur at the benzene ring.

Fluoranthene undergoes electrophilic substitution predominantly in the 3(4)-position, and additionally minor amounts of the 8(9)-substituted isomer are sometimes formed.<sup>27</sup> Few reactions involving the intermediacy of the radical cation of **5** have been performed, and it is therefore difficult to check the predictions above. The nucleophilic attack of trinitromethanide ion upon  $5^{+\bullet}$  has been probed in the photochemical addition of tetranitromethane to fluoranthene in dichloromethane at  $-20^\circ C$ .<sup>28</sup> This type of reaction has been shown<sup>29</sup> to occur *via* the photoinduced formation of a triad [ $5^{+\bullet}$  ( $NO_2$ )<sub>3</sub>C<sup>-</sup>  $NO_2$ ] from which initial attack of trinitromethanide ion upon  $5^{+\bullet}$  gives a neutral radical which is converted into an adduct by reaction with  $NO_2$ . The adduct isolated (**7**, 10% yield) was that formed from trinitromethanide attack at the 3-position; other, unknown adducts (9%) were also

**Table 4** Isomer distributions of the reaction between  $1^{+\bullet}$  and  $NO_2$ , as well as theoretical and experimental spin density distributions in  $1^{+\bullet}$

Reaction of $1^{+\bullet}$ with	Isomer distribution (%)				Ref.
	1-	2-	3-	4-	
$NO_2$ in $CH_2Cl_2$ ( $HNO_2$ catalysed nitration)	10	12	78	<0.1	9a
$NO_2$ in HFP <sup>a</sup> [ $h\nu$ with $C(NO_2)_4$ ]	6	9	71	14	66
Theoretical spin density distribution of ${}^2A_2$ state, normalized over positions 1-4	18	6	59	16	This work
Theoretical spin density distribution of ${}^2B_1$ state, normalized over positions 1-4	12	37	17	34	This work
Experimental spin density distribution, normalized over positions 1-4	25	1	67	7	30

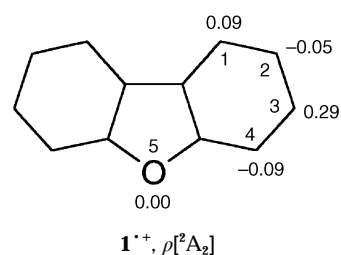
<sup>a</sup> 1,1,1,3,3,3-Hexafluoropropan-2-ol.



seen, and it is not presently known which remaining positions were attacked.

#### Radical cation-radical reactions and radical cation spin density

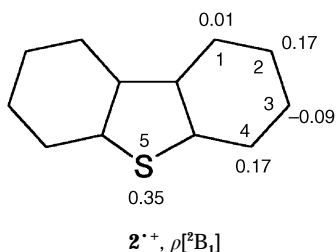
Further tests of the predictive power of the quantum chemical calculations is provided by the regioselectivity of radical cation-radical reactions of the systems studied, as well as the EPR spectral parameters of the radical cations. The calculated spin densities for the  ${}^2A_2$  state of  $1^{+\bullet}$  are shown below. The experimental determination<sup>30</sup> of the spin density distribution in  $1^{+\bullet}$  in a Freon matrix at 77 K (Table 4) suggests that *ca.* 70% of



the spin density resides in the 3-position which is only compatible with the calculated values for the  ${}^2A_2$  state (see Table 2).

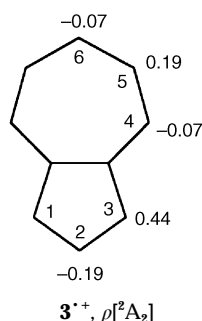
The reaction of  $1^{+\bullet}$  with a radical,  $NO_2$ , is an uncomplicated radical coupling reaction and its isomer distribution should follow the spin density distribution of the radical cation. From Table 4 it is seen that the  ${}^2A_2$  state of  $1^{+\bullet}$  (see above) is the one which adequately predicts the experimental spin density distribution and the isomer distribution from the  $1^{+\bullet}$ - $NO_2$  reaction. The  ${}^2B_1$  state (Table 2) puts the highest spin density at the 2- and 4-positions, which is contradicted by the experimental results.

For coupling between  $2^{+\bullet}$  and a radical, the spin density distribution of the  ${}^2B_1$  state would suggest predominant coupling at the 2- and 4-positions (below), in other words opposite orientation from that predicted for the  $2^{+\bullet}$ -Nu<sup>-</sup> reactions. In addition, the sulfur atom should be a major site of radical coupling. Here the CASPT2 method distinctly singles out the  ${}^2B_1$  state as the lowest one (difference 0.56 eV) so that the assignment appears to rest on solid ground. The EPR spectrum



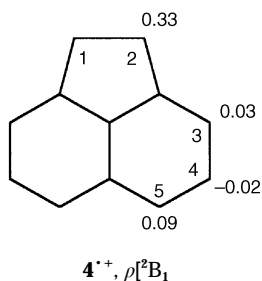
of the radical cation could not be resolved in earlier work,<sup>31</sup> but it was recently concluded from a study of the radical cations of dibenzothiophene and a series of methylsubstituted dibenzothiophenes that the spin density distribution of  $2^{+\bullet}$  indeed corresponds to that of the  ${}^2\text{B}_1$  state.<sup>32</sup>

Radical attack upon  $3^{+\bullet}$  should occur in the order of the



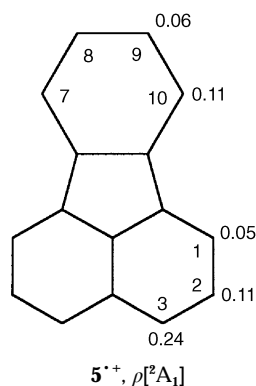
1(3)- > 5(7)-  $\approx$  2-positions, as shown below. This order agrees semiquantitatively with the hfs coupling constants<sup>33</sup> of the EPR spectrum of  $3^{+\bullet}$ : 1.07 [1(3)-] > 0.415 [5(7)-] > 0.152 (2-) > 0.112 (6-) > 0.038 [4(8)-] mT.

Radical attack upon  $4^{+\bullet}$  should occur predominantly at the



1(2)-position (see below). To our knowledge, the EPR spectrum of  $4^{+\bullet}$  has not been reported, nor do any  $4^{+\bullet}$ -radical reactions seem to be known.

Any  $5^{+\bullet}$ -radical reactions are predicted to occur in 2(5)-,



3(4)- and 7(10)-positions (see below). The nitration of **5** by  $\text{NO}_2$  in dichloromethane has been shown<sup>34</sup> to give a mixture of 3(4)- (69%), 8(9)- (23%), 7(10)- (3%), 2(5)- (2%) and 1(6)- (3%) nitro isomers [an earlier study<sup>35</sup> gave a similar result, 3(4)- (63%), 8(9)- (27%), other isomers (10%)]. This isomer distribution is

somewhat different from the isomer distribution from  $\text{NO}_2^+$  mediated nitration in  $\text{HNO}_3$ -acetic anhydride, 3(4)- (49%), 8(9)- (31%), 7(10)- (11%), 2(5)- (<0.5%) and 1(6)- (9%). Since the  $\text{NO}_2$  reaction is believed to be analogous to nitrous acid catalysed nitration which has the radical cation- $\text{NO}_2$  coupling step as the product-forming one,<sup>36</sup> its isomer distribution may be taken as a measure of the value of the prediction above, that  $5^{+\bullet}$ -radical reactions should occur in 1(6)-, 3(4)- and 7(10)-positions. Obviously, the 3(4)-position is the favoured one, but nitration in the 1(6)- and 7(10)-positions contributes only 6% together.

Attempts to obtain the fluid solution EPR spectrum of  $5^{+\bullet}$  so far have failed due to facile formation of the radical cation of 3,3'-bifluoranthene which had a persistent EPR spectrum.<sup>37</sup>

### Methods and theoretical considerations

The wave function and energy calculations were performed using the multiconfigurational SCF approach with dynamic electron correlation estimated by means of second order perturbational theory. This approach uses wave functions of the complete active space (CAS) type, which are characterized as a full configuration interaction (CI) in a set of active orbitals (in this case they will be  $\pi$ -orbitals).<sup>38</sup> All orbitals, inactive and active, are optimized (CASSCF). The wave function is a true spin eigenfunction in contrast to the unrestricted Hartree-Fock (UHF) wave function most commonly used to compute spin densities in organic radicals.

The energy calculations used the CASSCF wave function as the reference in a second order perturbation treatment of the remaining electron correlation energy (dynamic correlation).<sup>39,40</sup> This approach has been used to study the electronic spectra of a large number of molecules, radicals, cations and anions (for two recent reviews, see refs. 41 and 42). In general calculated excitation energies are accurate to better than 0.2–0.3 eV (*ca.* 2000  $\text{cm}^{-1}$ ) with basis sets of the quality used in the present work. The lowest triplet states normally have an accuracy of about 0.1 eV and this is the accuracy expected for the molecules treated here.

A crucial issue in the CASSCF/CASPT2 approach is the choice of active orbitals. It is determined by the types of excited states to be studied, in this case excitations within the  $\pi$ -electron space. Thus, the active space chosen included the valence  $\pi$ -orbitals with the  $\pi$ -electrons active. All  $\sigma$ -electrons were treated as inactive (doubly occupied in the CASSCF wave function), but were also correlated in the CASPT2 treatment. The core orbitals (1s in carbon and oxygen and 1s, 2s and 2p in sulfur) were kept frozen in the form determined by the ground state SCF functions and were not correlated.

The current implementation of the CASPT2 method limits the number of active orbitals to 12–14 depending on symmetry. The fluoranthene molecule (**5**) has 16 valence  $\pi$ -orbitals. This exceeds that limit in both the CASSCF and the CASPT2 programs. Therefore the four most stable orbitals (0301) were kept inactive, which leads to an active space of 12 orbitals (0606) with eight active electrons.<sup>43</sup> The acenaphthylene molecule (**4**) has 12 valence  $\pi$ -orbitals, while dibenzofuran (**1**) and dibenzothiophene (**2**) have 13, which is at the limit of what the CASPT2 program can handle. The lowest  $\pi$ -orbital is, however, well separated in energy from the others and full valence CASSCF calculations also give an occupation number close to two for this orbital of all three molecules. It was therefore decided to keep it inactive, leading to the following active spaces: (0606) for **1** and **2**, and (0605) for **4**.

A problem with the CASPT2 method is the appearance of intruder states. For low order non-degenerate perturbation theory to work, we demand that the reference function is well separated from the electronic states which are used to build the first-order wave function. This is normally achieved by including all near-degeneracy into the CASSCF space. Sometimes it may, however, happen that orbitals outside the active space give

rise to excitations nearly degenerate with the reference function. There are two possible ways to save the situation. One is to include the corresponding orbital into the active space. This was done in azulene **3** resulting in the active space (0704). Intruder states occur also in **1** and **2**. However, they are only weakly coupled and were removed by a newly introduced level shift technique.<sup>44</sup> A level shift value of 0.2 Hartree was used.

Basis sets of atomic natural orbital (ANO) type were used.<sup>45</sup> The number and types of contracted functions were selected on the basis of a systematic study of the influence of the basis sets on the excited states in the pyrazine molecule.<sup>46</sup> The contracted sets were S[4s3p1d], C,O[3s2p1d] and H[2s]. Basis sets of this quality were shown to give results that deviate at most by 0.1–0.2 eV from the large basis set results for the excitation energies in pyrazine. Fluoranthene represented the largest calculation with a total 234 basis functions. All calculations were performed at the experimental geometry.<sup>47</sup> The program MOLCAS,<sup>48</sup> versions 2 and 3, were used and the calculations were carried out on the IBM 9021/500-2VF computer at the University of Valencia.

Previous CASSCF calculations<sup>9a</sup> on **1** were made with the (0706) active space but a smaller ANO basis set: C,O[3s3p], H[2s]. With this active space the lowest electronic states of **1**<sup>•+</sup> were almost degenerate, with the <sup>2</sup>B<sub>1</sub> state 0.03 eV above the <sup>2</sup>A<sub>2</sub> state. The present CASSCF calculations, using the (0606) active space, where the lowest  $\pi$ -orbital is left inactive, increases this difference to 0.50 eV. The CASPT2 results reverse, however, the order and places the <sup>2</sup>B<sub>1</sub> state 0.06 eV below <sup>2</sup>A<sub>2</sub>. As was pointed out in the previous section, this is the wrong ordering, at least when judged from solution results. Photoelectron spectra show that the two states are almost degenerate which is in agreement with the results of the calculation.<sup>49</sup> The situation is different in **2**, where the difference between the two states is 0.5 eV. It is thus clear that the <sup>2</sup>B<sub>1</sub> state is the lowest cation state in **2** which makes its properties distinctly different from those of **1**.

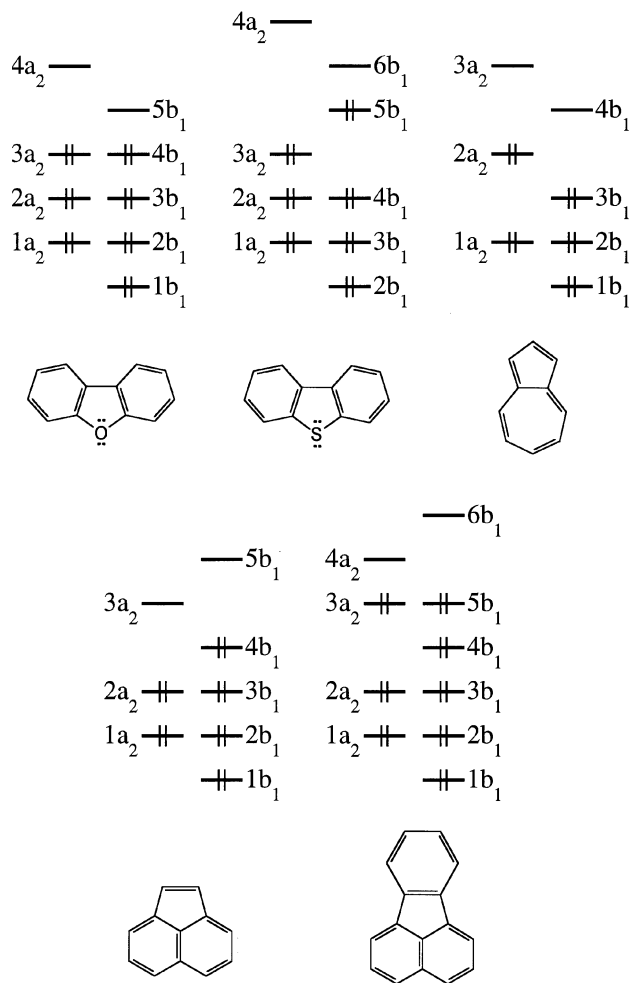
The results in Table 1 are also compared to experiment. We notice that all the triplet state energies are between 0.2 and 0.5 eV larger than the experimental ones. Calculated values correspond to vertical excitation energies at the geometry of the ground state, while the measured data are from phosphorescence emission. This explains the higher values of the computed excitation energies. The ionization energies are on the other hand between 0.1 and 0.5 eV smaller than the experimental data given in Table 1. This is due to the limited basis set used in the study. Larger basis sets are needed to account fully for the changes in electron correlation that takes place when an electron is removed from the system. The error is systematic, since there is a larger change in the ground state correlation energy.

#### CASPT2 orbital features of non-alternant radical cations and their relation to the VBCM model

The  $\pi$ -MOs of the non-alternant systems can be classified, according to the  $C_{2v}$  point group symmetry, as either of b<sub>1</sub> or a<sub>2</sub> types. Scheme 2 shows the occupied orbitals numbered in consecutive energy order for each set. For dibenzothiophene **2** account is taken also of the  $\pi$ -MO corresponding to the sulfur 2p orbital. Also shown in Scheme 2 are two orbitals which are vacant in the neutral hydrocarbon but become populated in the triplet states. These are the transfer orbitals (TOs) which are required for the VBCM analysis (e.g. Fig. 1 or Scheme 1b).

Typically the two highest occupied MOs are of the a<sub>2</sub> and b<sub>1</sub> symmetry and would give rise to two low-lying states, <sup>2</sup>A<sub>2</sub> and <sup>2</sup>B<sub>1</sub>, of the radical cation. These states are occasionally close in energy, and since  $C_{2v}$  symmetry is lost during the reaction, these states should mix significantly. Thus the ground state for the reactants, Nu:<sup>-</sup>/ArH<sup>•+</sup>, may well involve two configurations as opposed to the generic single configuration **a** in Scheme 1.

More complex is the configurational make-up of the triplet states. Based on Scheme 2, it is apparent that the target mol-



Scheme 2

ecules will possess two low-lying triplets, of the <sup>3</sup>B<sub>2</sub> and <sup>3</sup>A<sub>1</sub> types: <sup>3</sup>B<sub>2</sub> arises from a<sub>2</sub> → b<sub>1</sub>/b<sub>1</sub> → a<sub>2</sub> excitations, while <sup>3</sup>A<sub>1</sub> arises from a<sub>2</sub> → a<sub>2</sub>/b<sub>1</sub> → b<sub>1</sub> excitations. The multiconfigurational nature of the triplet, as well as their possible mixing clearly deviate from the generic picture of configuration **b** in Scheme 1. It is therefore important to establish a connection between the complex electronic structure and the simple generic picture of two VB configurations, each described by a unique electronic structure in Scheme 1. Table 5 shows the coefficients of the leading CASSCF configurations for the ground state(s) of the radical cation and the <sup>3</sup>B<sub>2</sub> and <sup>3</sup>A<sub>1</sub> triplet states. It is seen that the leading configurations have substantial weights which are much larger than the splinter weights of the remaining configurations. As such, we can use these leading CASPT2 configurations to represent the VB mixing in our problem. The minor configurations will always mix in so as to maximize the bonding due to the leading configuration mixing.<sup>4a</sup>

The matrix elements between the reactant configuration Nu:<sup>-</sup>/ArH<sup>•+</sup> (**a**, Scheme 1) and the excited one, Nu:<sup>-</sup>/<sup>3</sup>(ArH) (**b**, Scheme 1) involve the resonance integral between the nucleophile orbital (n) and the 'LUMO' of the radical cation. This 'LUMO' is referred to in the text as the transfer orbital (TO). The TO is seen from Scheme 1 to be singly occupied in the excited state configuration (**b**). The TO is optimized in the CASSCF procedure and thus its coefficients are meaningful. This is why we use, throughout, the TO coefficients and not 'LUMO' coefficients. Of course, if one uses non-SCF orbitals such as Hückel MOs the TO and the LUMO are identical orbitals, and one may use the Hückel LUMOs coefficients to make predictions.

Table 6 shows these matrix elements between the leading CASSCF configurations which describe the VBCM of Nu:<sup>-</sup>/

**Table 5** Weights of leading CASPT2 configurations for radical cations and triplet states of 1–5

Species	State <sup>a,b</sup>	Electronic structure <sup>c</sup>	CI coefficient
<b>1</b>	<sup>2</sup> A <sub>2</sub>	(1b <sub>1</sub> <sup>2</sup> 2b <sub>1</sub> <sup>2</sup> 1a <sub>2</sub> <sup>2</sup> 3b <sub>1</sub> <sup>2</sup> 2a <sub>2</sub> <sup>2</sup> )4b <sub>1</sub> <sup>2</sup> 3a <sub>2</sub> <sup>1</sup>	0.89
	<sup>2</sup> B <sub>1</sub>	( )4b <sub>1</sub> <sup>1</sup> 3a <sub>2</sub> <sup>2</sup>	0.88
	<sup>3</sup> B <sub>2</sub>	( )4b <sub>1</sub> <sup>2</sup> 3a <sub>2</sub> <sup>1</sup> 5b <sub>1</sub> <sup>1</sup>	0.75 <sup>d</sup>
	<sup>3</sup> A <sub>1</sub>	( )3a <sub>2</sub> <sup>2</sup> 4b <sub>1</sub> <sup>1</sup> 5b <sub>1</sub> <sup>1</sup>	0.63 <sup>d</sup>
<b>2</b>	<sup>2</sup> A <sub>2</sub>	[1b <sub>1</sub> <sup>2</sup> 2b <sub>1</sub> <sup>2</sup> 1a <sub>2</sub> <sup>2</sup> 3b <sub>1</sub> <sup>2</sup> 3a <sub>2</sub> <sup>2</sup> 4b <sub>1</sub> <sup>2</sup> 2a <sub>2</sub> <sup>2</sup> 4a <sub>2</sub> <sup>1</sup>	0.51 <sup>d</sup>
	<sup>2</sup> B <sub>1</sub>	(1b <sub>1</sub> <sup>2</sup> 2b <sub>1</sub> <sup>2</sup> 1a <sub>2</sub> <sup>2</sup> 4b <sub>1</sub> <sup>2</sup> 2a <sub>2</sub> <sup>2</sup> )5b <sub>1</sub> <sup>2</sup> 3a <sub>2</sub> <sup>1</sup>	0.89
	<sup>3</sup> B <sub>2</sub>	( )5b <sub>1</sub> <sup>1</sup> 3a <sub>2</sub> <sup>2</sup>	0.90
	<sup>3</sup> A <sub>1</sub>	( )5b <sub>1</sub> <sup>2</sup> 3a <sub>2</sub> <sup>1</sup> 6b <sub>1</sub> <sup>1</sup>	0.78 <sup>d</sup>
<b>3</b>	<sup>2</sup> A <sub>2</sub>	( )3a <sub>2</sub> <sup>2</sup> 5b <sub>1</sub> <sup>1</sup> 6b <sub>1</sub> <sup>1</sup>	0.64 <sup>d</sup>
	<sup>2</sup> B <sub>1</sub>	[( )5b <sub>1</sub> <sup>2</sup> 3a <sub>2</sub> <sup>1</sup> 4a <sub>2</sub> <sup>1</sup>	–0.51 <sup>d</sup>
	<sup>3</sup> B <sub>2</sub>	(1b <sub>1</sub> <sup>2</sup> 2b <sub>1</sub> <sup>2</sup> 3b <sub>1</sub> <sup>2</sup> 1a <sub>2</sub> <sup>2</sup> )2a <sub>2</sub> <sup>1</sup>	0.89
	<sup>3</sup> A <sub>1</sub>	(1b <sub>1</sub> <sup>2</sup> 2b <sub>1</sub> <sup>2</sup> 1a <sub>2</sub> <sup>2</sup> 2a <sub>2</sub> <sup>2</sup> )3b <sub>1</sub> <sup>1</sup>	0.89
<b>4</b>	<sup>2</sup> A <sub>2</sub>	( )2a <sub>2</sub> <sup>1</sup> 4b <sub>1</sub> <sup>1</sup>	0.75 <sup>d</sup>
	<sup>2</sup> B <sub>1</sub>	( )2a <sub>2</sub> <sup>1</sup> 3a <sub>2</sub> <sup>1</sup>	0.75 <sup>d</sup>
	<sup>3</sup> B <sub>2</sub>	[( )3b <sub>1</sub> <sup>1</sup> 4b <sub>1</sub> <sup>1</sup>	0.43 <sup>d</sup>
	<sup>3</sup> A <sub>1</sub>	(1b <sub>1</sub> <sup>2</sup> 2b <sub>1</sub> <sup>2</sup> 3b <sub>1</sub> <sup>2</sup> 4b <sub>1</sub> <sup>2</sup> 1a <sub>2</sub> <sup>2</sup> )2a <sub>2</sub> <sup>1</sup>	0.89
<b>5</b>	<sup>2</sup> A <sub>2</sub>	(1b <sub>1</sub> <sup>2</sup> 2b <sub>1</sub> <sup>2</sup> 3b <sub>1</sub> <sup>2</sup> 1a <sub>2</sub> <sup>2</sup> 2a <sub>2</sub> <sup>2</sup> )4b <sub>1</sub> <sup>1</sup> 3a <sub>2</sub> <sup>1</sup>	0.90
	<sup>2</sup> B <sub>1</sub>	(1b <sub>1</sub> <sup>2</sup> 2b <sub>1</sub> <sup>2</sup> 3b <sub>1</sub> <sup>2</sup> 1a <sub>2</sub> <sup>2</sup> 2a <sub>2</sub> <sup>2</sup> )4b <sub>1</sub> <sup>1</sup>	0.90
	<sup>3</sup> B <sub>2</sub>	(1b <sub>1</sub> <sup>2</sup> 2b <sub>1</sub> <sup>2</sup> 3b <sub>1</sub> <sup>2</sup> 1a <sub>2</sub> <sup>2</sup> 2a <sub>2</sub> <sup>2</sup> )4b <sub>1</sub> <sup>1</sup> 3a <sub>2</sub> <sup>1</sup>	0.87 <sup>d</sup>
	<sup>3</sup> A <sub>1</sub>	(1b <sub>1</sub> <sup>2</sup> 2b <sub>1</sub> <sup>2</sup> 3b <sub>1</sub> <sup>2</sup> 4b <sub>1</sub> <sup>2</sup> 1a <sub>2</sub> <sup>2</sup> )2a <sub>2</sub> <sup>2</sup> 3a <sub>2</sub> <sup>1</sup>	0.83
<b>5</b>	<sup>2</sup> A <sub>2</sub>	[(1b <sub>1</sub> <sup>2</sup> 2b <sub>1</sub> <sup>2</sup> 3b <sub>1</sub> <sup>2</sup> 1a <sub>2</sub> <sup>2</sup> 2a <sub>2</sub> <sup>2</sup> )4b <sub>1</sub> <sup>1</sup> 5b <sub>1</sub> <sup>1</sup> ]	–0.24]
	<sup>2</sup> B <sub>1</sub>	(1b <sub>1</sub> <sup>2</sup> 2b <sub>1</sub> <sup>2</sup> 3b <sub>1</sub> <sup>2</sup> 4b <sub>1</sub> <sup>2</sup> 5b <sub>1</sub> <sup>2</sup> 1a <sub>2</sub> <sup>2</sup> 2a <sub>2</sub> <sup>2</sup> )3a <sub>2</sub> <sup>1</sup>	0.94
	<sup>3</sup> B <sub>2</sub>	(1b <sub>1</sub> <sup>2</sup> 2b <sub>1</sub> <sup>2</sup> 3b <sub>1</sub> <sup>2</sup> 4b <sub>1</sub> <sup>2</sup> 1a <sub>2</sub> <sup>2</sup> 2a <sub>2</sub> <sup>2</sup> 3a <sub>2</sub> <sup>2</sup> )5b <sub>1</sub> <sup>1</sup>	0.90
	<sup>3</sup> A <sub>1</sub>	(1b <sub>1</sub> <sup>2</sup> 2b <sub>1</sub> <sup>2</sup> 3b <sub>1</sub> <sup>2</sup> 4b <sub>1</sub> <sup>2</sup> 1a <sub>2</sub> <sup>2</sup> 2a <sub>2</sub> <sup>2</sup> 3a <sub>2</sub> <sup>2</sup> )4a <sub>1</sub> <sup>1</sup> 5b <sub>1</sub> <sup>1</sup>	0.85
		(1b <sub>1</sub> <sup>2</sup> 2b <sub>1</sub> <sup>2</sup> 3b <sub>1</sub> <sup>2</sup> 4b <sub>1</sub> <sup>2</sup> 5b <sub>1</sub> <sup>2</sup> 1a <sub>2</sub> <sup>2</sup> 2a <sub>2</sub> <sup>2</sup> )3a <sub>2</sub> <sup>1</sup> 4a <sub>2</sub> <sup>1</sup>	0.91

<sup>a</sup> <sup>2</sup>A<sub>2</sub> and <sup>3</sup>B<sub>2</sub> are the radical cation, ArH<sup>•+</sup>, states: <sup>3</sup>B<sub>2</sub> and <sup>3</sup>A<sub>1</sub> are the triplet states, <sup>3</sup>(ArH). <sup>b</sup> The relative energies of the states are given in Table 1. <sup>c</sup> These are the leading configurations. <sup>d</sup> There are other configurations with weights of 0.05–0.1.

**Table 6** Matrix elements<sup>a</sup> between leading CASSCF configurations in the reactant ( $\Psi_R$ ) and excited ( $\Psi_P$ ) configurations

Reactant configuration	$\Psi_P(1); ^3B_2$	$\Psi_P(2); ^3A_1^b$
Dibenzofuran ( <b>1</b> )		
$\Psi_R(1); ^2A_2$	$\langle n   5b_1 \rangle$	$\langle n, 5b_1   4b_1, 3a_2 \rangle$
$\Psi_R(2); ^2B_1$	$\langle n, 5b_1   4b_1, 3a_2 \rangle$	$\langle n   5b_1 \rangle$
Dibenzothiophene ( <b>2</b> )		
$\Psi_R(1); ^2A_2$	$\langle n   6b_1 \rangle$	$\langle n, 6b_1   5b_1, 3a_2 \rangle$
$\Psi_R(2); ^2B_1$	$\langle n, 6b_1   5b_1, 3a_2 \rangle$	$\langle n   6b_1 \rangle$
Azulene ( <b>3</b> )		
$\Psi_R(1); ^2A_2$	$\langle n   4b_1 \rangle$	$\langle n   3a_2 \rangle$
$\Psi_R(2); ^2B_1$	—	—
Acenaphthylene ( <b>4</b> )		
$\Psi_R(1); ^2A_2$	$\langle n, 3a_2   4b_1, 3a_2 \rangle$	$\langle n   3a_2 \rangle$
$\Psi_R(2); ^2B_1$	$\langle n   3a_2 \rangle$	$\langle n, 3a_2   4b_1, 3a_2 \rangle$
Fluoranthene ( <b>5</b> )		
$\Psi_R(1); ^2A_2$	$\langle n, 4a_2   5b_1, 3a_2 \rangle$	$\langle n   4a_2 \rangle$
$\Psi_R(2); ^2B_1$	$\langle n   4a_2 \rangle$	$\langle n, 4a_2   5b_1, 3a_2 \rangle$

<sup>a</sup> n is the HOMO of Nu<sup>•-</sup> (Scheme 1). The ArH orbitals are designated according to Scheme 2. One- and two-electron matrix elements are used. Only the orbitals involved are specified, not the detailed form of the matrix element. <sup>b</sup> Only the major <sup>3</sup>A<sub>1</sub> component is used. Usually, only this component has a non-vanishing matrix element with  $\Psi_R(1)$ .

ArH<sup>•+</sup> and Nu<sup>•-</sup>/<sup>3</sup>(ArH) (see Fig. 1 and Scheme 1). There are four configurations nascent from the <sup>2</sup>A<sub>2</sub>, <sup>2</sup>B<sub>1</sub> states of ArH<sup>•+</sup> and the <sup>3</sup>B<sub>2</sub> and <sup>3</sup>A<sub>1</sub> states of <sup>3</sup>(ArH). The states are numbered 1–4 as specified in Scheme 3 where the two excited configurations are labelled as  $\Psi_P$ , indicating their correlation to the product of the addition reaction (Fig. 1). It is apparent from Table 6 that irrespective of whether the ground state is  $\Psi_R(1)(^2A_2)$  or  $\Psi_R(2)(^2B_1)$ , and whether the excited state is  $\Psi_P(1)(^3B_2)$  or  $\Psi_P(2)(^3A_1)$ , the coupling matrix element is invariably controlled by the overlap of the nucleophile orbital (n) with the TO which is the 'LUMO' of ArH. Consider for example, the matrix elements for dibenzofuran(1):  $\langle n | 5b_1 \rangle$  is a one-electronic matrix element, while  $\langle n, 5b_1 | 4b_1, 3a_2 \rangle$  is a two-electron matrix element. In both cases the overlap of n with the

**Table 7** Transfer orbital (TO) coefficients and corresponding SDD indices for 1–5

System	Site <sup>a</sup>	TO coefficients <sup>b</sup>	SDD <sup>c</sup>	Preferred sites for nucleophilic attack
<b>1</b>	1	0.45	0.22	3 ≈ 1 > 4 > 2
	2	0.06	–0.05	
	3	–0.53	0.10	
	4	0.30	0.17	
	5	–0.15	0.00	
<b>2</b>	1	0.43	0.30	3 > 1 > 4
	2	0.07	–0.23	
	3	–0.54	0.50	
	4	0.25	–0.14	
	5	–0.22	–0.33	
<b>3</b>	2	0.35	0.11	6 > 4
	3	–0.04	0.03	
	4	0.66	0.33	
	5	0.16	–0.20	
	6	–0.75	0.49	
<b>4</b>	2	0.69	0.24	2 ≈ 3 > 5
	3	–0.56	0.31	
	4	–0.08	–0.12	
	5	0.49	0.23	
<b>5</b>	1	–0.31	0.04	3 > 1 ≈ 2
	2	–0.41	0.01	
	3	0.63	0.11	
	9	0.17	0.00	
	10	–0.20	–0.07	

<sup>a</sup> Only symmetry unique sites are indicated. <sup>b</sup> The TO is the orbital in the matrix element between  $\Psi_R$  and  $\Psi_P$  (Table 6) of the lowest energies for each species. <sup>c</sup> The SDD refers to the difference in spin density between the lowest radical cation and triplet states of 1–5.

5b<sub>1</sub> TO determines the value of the matrix element, which is maximized when n overlaps with the dibenzofuran site of the highest TO (5b<sub>1</sub>) coefficient. Thus, in fact all the matrix elements in Table 6 follow the generic matrix elements discussed in the text. The regiochemical rule due to the avoided crossing interaction in Fig. 1 survives intact as long as we consider the leading configurations resulting from the CASSCF study.

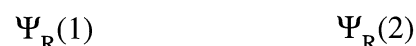
Thus, the regioselectivity will depend on the highest coefficient of the TO which is calculated by the CASSCF procedure. An alternative to the use of TO coefficients is the spin density difference (SDD) between the triplet state and the radical cation state. The SDD distribution at the various sites gauges the strength of the interaction at these sites, in an equivalent manner to the matrix element. When all the states share the same set of orbitals the SDD is simply the spin density of the TO. However, when the states have different orbitals the SDD and TO coefficients may give different predictions. For comparison we show in Table 7 both indices for the various systems using the lowest states of the radical cation and the triplet state to derive both indices. With the exception of **1** where the TO favours C-3 and C-4 attack while SDD favours C-4 over C-3 attack, in the rest of the systems both measures of regioselectivity lead to the same predicted trends. Therefore, we shall use in the text the TO coefficients to retain the original spirit of the VBCM model. We do, however, caution that the SDD indices are theoretically more meaningful as long as one uses CASSCF to derive reactivity indices because SDD is independent of the orbital representation. Clearly, a full treatment of the avoided crossing interaction *via* CASSCF would have led directly to the requisite *B* values at the various sites.

Let us go back to Table 6 to discuss the issue of the multi-configurational nature of  $\Psi_R$  and  $\Psi_P$  (Scheme 3) as opposed to the generic configurations (Scheme 1). Dibenzofuran radical cation (**1**<sup>•+</sup>) has virtually degenerate <sup>2</sup>A<sub>2</sub> and <sup>2</sup>B<sub>1</sub> states, while the triplet states are well separated, <sup>3</sup>B<sub>2</sub> being the lowest. Thus, a proper description of the ground state configuration would be  $\Psi_R(1) \pm \Psi_P(2)$ , while  $\Psi_P(1)$  will describe the excited configuration. It is apparent from Table 6 that the dominant matrix



**Table 8** Indices for predicting the regioselectivity of  $\text{Nu}^- + \text{ArH}^+ \longrightarrow \text{NuAr}^+(\text{H})$ , using the CASSCF results

Radical cation	TO	Triplet density
$1^{+\bullet}$	5b <sub>1</sub>	$\rho[{}^3\text{B}_2]$
$2^{+\bullet}$	6b <sub>1</sub>	$\rho[{}^3\text{B}_2]$
$3^{+\bullet}$	4b <sub>1</sub> (main) 3a <sub>2</sub> (secondary)	$\rho[{}^3\text{B}_2]$ (main) $\rho[{}^3\text{A}_1]$ (secondary)
$4^{+\bullet}$	3a <sub>2</sub>	$\rho[{}^3\text{B}_2]$ (main)
$5^{+\bullet}$	4a <sub>2</sub>	$\rho[{}^3\text{A}_1]$ (main) $\rho[{}^3\text{A}_1]$ (secondary)



**Scheme 3**

element depends on the 5b<sub>1</sub> TO, irrespective of the nature of  $\Psi_{\text{R}}$ . The regioselectivity for nucleophilic attack on  $1^{+\bullet}$  will be determined by the combination of the 5b<sub>1</sub> TO coefficients and the  ${}^3\text{B}_2$  spin density ( $\rho[{}^3\text{b}_2]$ ) distribution, as summarized in Table 8.

For dibenzothiophene radical cation ( $2^{+\bullet}$ ), the ground state of the radical cation is  ${}^2\text{B}_1$  and the lowest triplet state is  ${}^3\text{B}_2$ . Both states are well separated from their next high counterparts. The corresponding predictors are shown in Table 8. For azulene radical cation ( $3^{+\bullet}$ )  ${}^2\text{A}_2$  is the lowest radical cation state. The triplet states are more closely spaced,  ${}^3\text{B}_2$  being the lowest. Accordingly, the main predictors are the 4b<sub>1</sub> TO and  $\rho[{}^3\text{B}_2]$ , while 3a<sub>2</sub>-TO and  $\rho[{}^3\text{A}_1]$  will have a secondary influence. The 4b<sub>1</sub> TO predicts attack in the order of C-6 > C-4 ≫ C-2, while  $\rho[{}^3\text{B}_2]$  predicts attack in the order of C-6 > C-2 > C-4. The secondary TO, 3a<sub>2</sub> and  $\rho[{}^3\text{A}_1]$  give preference to attack at C-4 and C-2, so that a weighted prediction seems to be C-6 > C-4, C-2. This differs somewhat from that based on the main predictors.

For acenaphthylene radical cation ( $4^{+\bullet}$ ) the relevant ground states are  ${}^2\text{B}_1$  and  ${}^3\text{B}_2$  which are separated by 0.4 eV from their analogous  ${}^2\text{A}_2$  and  ${}^3\text{A}_1$  states. Based on this separation the regioselectivity predictors in Table 8 are the 3a<sub>2</sub>-TO and  $\rho[{}^3\text{B}_2]$ . Using  ${}^2\text{B}_1 \pm {}^2\text{A}_2$  for the ground states does not change the TO, much as the use of  ${}^3\text{B}_2 \pm {}^3\text{A}_1$  for the excited state. Using  $\rho[{}^3\text{A}_1]$  as a secondary predictor raises the regioselectivity of C-5 over C-3, thus making the net prediction C-1 > C-3 ~ C-5. Nonetheless, one must remember that attack on C-1 is preferred also thermodynamically [see  $\Delta E_{\text{RP}}$  in eqn. (2) in the text] so that it should dominate the chemistry of acenaphthylene.

The appropriate ground states of fluoranthene (**5**) are  ${}^2\text{A}_2$  and  ${}^3\text{A}_1$ . Based on these, the predictors in Table 8 are 4a<sub>2</sub>-TO and  $\rho[{}^3\text{a}_1]$ . Taking linear combination states with  ${}^2\text{B}_1$  and  ${}^3\text{B}_2$  will not alter the dominant TO. However, the spin density of  ${}^3\text{B}_2$  ( $\rho[{}^3\text{B}_2]$ ) will prefer C-3(4) positions over C-1(6), such that the selectivity for attack will be C-3 > C-1 > C-2.

The multiconfigurational nature does not, after all, drastically change the specific predictions which are reached by considering the leading configurations. Since the latter are analogous to the generic VBCM model (Fig. 1, Scheme 1) the predictions used in the text are based on the leading configurations generated from the consideration of the ground states for the radical cation ( ${}^2\text{A}_2$  or  ${}^2\text{B}_1$ ) and the lowest triplet state of

ArH ( ${}^3\text{B}_2$  or  ${}^3\text{A}_1$ ). Even though the deviations from the generic picture are not drastic, there are nevertheless deviations. This is apparent from the differences in TO coefficients and SDDs (Table 7) and the modification introduced by the multiconfigurational character of the initial states. It is not easy to assess the effect of these deviations on the strength of the regiochemical predictions in the text. In this sense, the interplay of experiment and theory will be extremely fruitful in outlining the limitations of the simple theory and the directions in which it might be modified.

## Conclusions

This paper couples the VBCM model with a sophisticated quantum chemical method, CASPT2, to generate reactivity predictors for the regioselectivity of nucleophilic attack on radical cations,  $\text{Nu}^- + \text{ArH}^+$ . Based on a generic VBCM model with two configurations (Scheme 1), the nucleophilic attack is predicted to occur on those ArH sites which possess the highest spin density in the triplet  ${}^3(\text{ArH})$  species and the largest coefficient in the transfer orbital (TO) of  $\text{ArH}^+$ . The TO is formally the  $\text{ArH}^+$  LUMO which becomes singly occupied in  ${}^3(\text{ArH})$ , as the configurations  $\text{Nu}^-/\text{ArH}^+$  and  $\text{Nu}^\bullet/{}^3(\text{ArH})$  cross along the reaction coordinate (Fig. 1).

A careful analysis of the CASPT2 configurations shows that the predictions of the generic model are not altered drastically when more configurations are used to model the curve crossing. Thus, even though deviations are expected (see Methods), the primary regioselectivities predicted by the generic model survive upon inclusion of additional configurations. The ability of the CASPT2 method to generate reactivity indices is demonstrated for radical attacks on the radical cations used in our study. Thus the reactivity indices derived from CASPT2 for the corresponding nucleophilic attacks should be considered as reliable electronic factors of the problem within its VBCM modelling.

The scarce experimental data (e.g. see Table 1 for  $\text{Nu}^-/1^{+\bullet}$ ) compare favourably with the VBCM/CASPT2 predictions. However, most of the predictions will require experimental testing which can serve to refine the model and our understanding of the subtle problem of the regioselectivity of nucleophilic attack upon radical cations.

## Acknowledgements

Financial support from the Swedish Natural Science Research Council (to L. E. and B. O. R.) and by the Spanish Project No. PB94-0986 (to R. G.-L. and M. M.) is gratefully acknowledged. The research at the Hebrew University is supported by the Volkswagen Stiftung.

## References

- For reviews on radical cation reactivity, see: O. Hammerich and V. D. Parker, *Adv. Phys. Org. Chem.*, 1984, **20**, 55; A. J. Bard, A. Ledwith and H. J. Shine, *Adv. Phys. Org. Chem.*, 1976, **12**, 155.
- L. Ebersson, Z. Blum, B. Helg e and K. Nyberg, *Tetrahedron*, 1978, **34**, 731; L. Ebersson and K. Nyberg, *Acta Chem. Scand., Ser. B*, 1978, **32**, 235.
- A. Pross, *J. Am. Chem. Soc.*, 1986, **110**, 3537.
- (a) S. S. Shaik, *J. Am. Chem. Soc.*, 1982, **103**, 3692; (b) A. Pross, *Adv. Phys. Org. Chem.*, 1985, **21**, 99; (c) S. S. Shaik, *Progr. Phys. Org. Chem.*, 1985, **15**, 197; (d) A. Pross and S. S. Shaik, *Acc. Chem. Res.*, 1983, **110**, 3537.
- See, e.g.: (a) V. D. Parker, B. Reitst en and M. Tilset, *J. Phys. Org. Chem.*, 1989, **2**, 580; (b) B. Reitst en, F. Norrsell and V. D. Parker, *J. Am. Chem. Soc.*, 1989, **111**, 8463; (c) T. Drewello, N. Heinrich, N. W. M. P. Mass, N. M. M. Nibbering, T. Weiske and H. Schwarz, *J. Am. Chem. Soc.*, 1987, **109**, 4810; (d) J. P. Dinnocenzo, S. Farid, S. J. L. Goodman, I. R. Gould and W. P. Todd, *Mol. Cryst. Liq. Cryst.*, 1991, **194**, 151.
- (a) S. S. Shaik and A. Pross, *J. Am. Chem. Soc.*, 1989, **111**, 4306; (b) S. S. Shaik and J. P. Dinnocenzo, *J. Org. Chem.*, 1990, **55**, 3434; (c) S. Shaik, A. C. Reddy, A. Ioffe, J. P. Dinnocenzo, D. Danovich and J. K. Cho, *J. Am. Chem. Soc.*, 1995, **117**, 3205.

- 7 The EA(ketene<sup>+</sup>) used in ref. 6(a) is apparently in error. The correct value should be ca. 221 kcal mol<sup>-1</sup>. For a revised *B* value, see ref. 6(c).
- 8 B. O. Roos, P. R. Taylor and P. E. Siegbahn, *Chem. Phys.*, 1980, **48**, 157.
- 9 (a) L. Ebersson, M. P. Hartshorn, F. Radner, M. Merchán and B. O. Roos, *Acta Chem. Scand.*, 1993, **47**, 176; (b) L. Ebersson and F. Radner, *Acta Chem. Scand.*, 1992, **46**, 312; (c) L. Ebersson and F. Radner, *Acta Chem. Scand.*, 1992, **46**, 802.
- 10 For anodic substitution reactions, see K. Yoshida, *Electrooxidation in Organic Chemistry. The Role of Cation Radicals as Synthetic Intermediates*, Wiley, New York, 1984. For metal ion promoted acetoxylation, see L. Ebersson, *Electron Transfer Reactions in Organic Chemistry*, Springer, Heidelberg, 1987, pp. 80–82.
- 11 M. J. S. Dewar and R. C. Dougherty, *The PMO Theory of Organic Chemistry*, Plenum Press, New York, 1975, p. 75.
- 12 As explained in ref. 6(c) this curve crossing does not occur for cases where the nucleophile is neutral and has a high ionization potential. Even so, the VB mixing will involve the same configuration types.
- 13 S. S. Shaik, H. B. Schlegel and S. Wolfe, *Theoretical Aspects of Physical Organic Chemistry. Application to the S<sub>N</sub>2 Transition State*, Wiley, New York, 1992, ch. 3, 6.
- 14 (a) S. S. Shaik and E. Canadell, *J. Am. Chem. Soc.*, 1990, **112**, 1452; (b) S. S. Shaik and P. C. Hiberty, in *Theoretical Concepts for Chemical Bonding*, ed. A. B. Maksic, Springer, Heidelberg, 1991, vol. 4, pp. 324–378; (c) note in (a) that only when the stability differs markedly does the regioselectivity follow strictly the relative stability of the isomers.
- 15 The orbitals of these configurations correspond to the situation at the crossing point. These are effective configurations which include the effect of other configurations through the adaptation of the orbitals to the requisite mixing at the transition state. For discussions, see: (a) S. Shaik, in *New Theoretical Concepts for Understanding Organic Reactions*, eds. J. Bertran and I. G. Csizmadia, NATO ASI Series, Vol. C. 267, Kluwer, Netherlands, 1989, pp. 165–217; (b) S. Shaik and P. C. Hiberty, *Adv. Quant. Chem.*, 1995, **26**, 99.
- 16 R. Taylor, *J. Chem. Soc. B*, 1968, 1559.
- 17 A. R. Katritzky and R. Taylor, *Adv. Heterocyclic Chem.*, 1990, **47**, 181.
- 18 G. Bontempelli, F. Magno, G.-A. Mazzocchini and S. Zecchin, *J. Electroanal. Chem.*, 1973, **43**, 377.
- 19 R. Taylor, *Electrophilic Aromatic Substitution*, Wiley, New York, 1990, p. 67, 117.
- 20 V. A. Nefedev, N. A. German and G. I. Nikishin, *J. Org. Chem. USSR (Engl. Transl.)*, 1983, **19**, 1123.
- 21 V. A. Nefedev, L. K. Tarygina, L. V. Kruchkova and Yu. S. Ryabokobylko, *J. Org. Chem. USSR (Engl. Transl.)*, 1981, **17**, 487.
- 22 R. Zahradnik, in *Non-benzenoid Aromatics*, ed. J. P. Snyder, vol. II, Academic Press, New York, 1971, ch. 1 and references cited therein.
- 23 C. Rav-Acha, E. Choshen and S. Sarel, *Helv. Chim. Acta*, 1986, **69**, 1728.
- 24 B. Rindone and C. Scolastico, *Tetrahedron Lett.*, 1973, 1479.
- 25 W. S. Trahanovsky and M. D. Robbins, *J. Am. Chem. Soc.*, 1971, **93**, 5256.
- 26 E. Baciocchi, C. Rol and M. Mandolini, *J. Am. Chem. Soc.*, 1980, **102**, 7598.
- 27 Ref. 19, p. 98, 103, 404.
- 28 L. Ebersson, M. P. Hartshorn, F. Radner and W. T. Robinson, *Acta Chem. Scand.*, 1993, **47**, 410.
- 29 For reviews, see: (a) L. Ebersson, M. P. Hartshorn and F. Radner, *Acta Chem. Scand.*, 1994, **48**, 937; (b) L. Ebersson, M. P. Hartshorn and F. Radner, in *Advances in Carbocation Chemistry*, vol. 2, JAI Press, 1995, 207–263.
- 30 L. Ebersson, M. P. Hartshorn, O. Persson, F. Radner and C. J. Rhodes, *J. Chem. Soc., Perkin Trans 2*, 1996, 1289.
- 31 M. C. Depew, L. Zhongli and J. K. S. Wan, *J. Am. Chem. Soc.*, 1983, **105**, 2480.
- 32 L. Ebersson, M. P. Hartshorn, O. Persson and F. Radner, *Acta Chem. Scand.*, 1997, **51**, in the press.
- 33 R. M. Dessau and S. Shih, *J. Chem. Phys.*, 1970, **53**, 3169.
- 34 G. L. Squadrito, D. F. Church and W. A. Pryor, *J. Am. Chem. Soc.*, 1987, **109**, 6535.
- 35 F. Radner, *Acta Chem. Scand., Ser. B*, 1983, **37**, 65.
- 36 (a) L. Ebersson and F. Radner, *Acc. Chem. Res.*, 1987, **20**, 51; (b) J. H. Ridd, *Chem. Soc. Rev.*, 1991, **20**, 149; (c) E. Bosch and J. K. Kochi, *J. Org. Chem.*, 1994, **59**, 3314, 5573.
- 37 L. Ebersson and O. Persson, unpublished results.
- 38 B. O. Roos, *The complete active space self-consistent field method and its application in electronic structure calculations*, in ed., K. P. Lawley, *Advances in Chemical Physics; Ab Initio Methods in Quantum Chemistry-II*, Wiley, Chichester, England, 1987, ch. 69, p. 399.
- 39 K. Andersson, P.-Å. Malmqvist, B. O. Roos, A. J. Sadlej and K. Wolinski, *J. Phys. Chem.*, 1990, **94**, 5483.
- 40 K. Andersson, P.-Å. Malmqvist and B. O. Roos, *J. Phys. Chem.*, 1992, **96**, 1218.
- 41 B. O. Roos, M. P. Fülcher, P.-Å. Malmqvist, M. Merchán and L. Serrano-Andrés, *Theoretical studies of electronic spectra of organic molecules*, ed. S. R. Langhoff, *Quantum Mechanical Electronic Structure Calculations with Chemical Accuracy*, Kluwer, Dordrecht, 1995.
- 42 B. O. Roos, M. P. Fülcher, P.-Å. Malmqvist, M. Merchán, L. Serrano-Andrés and K. Pierlot, *Multiconfigurational perturbation theory: Applications in electronic spectroscopy*, in ed. S. A. Rice, *Advances in Chemical Physics: New Methods in Computational Quantum Mechanics*, Vol. XCIII:219, Wiley, New York, 1995.
- 43 The active space is labelled (*klmn*), where the indices give the number of active orbitals in the four irreducible representations of the C<sub>2v</sub> point group in the order a<sub>1</sub>, b<sub>1</sub>, b<sub>2</sub> and a<sub>2</sub>, respectively. The molecules are placed in the yz plane. Therefore the second and fourth symmetries correspond to π-orbitals.
- 44 B. O. Roos and K. Andersson, *Chem. Phys. Lett.*, 1995, **245**, 215.
- 45 K. Pierlot, B. Dumez, P.-O. Widmark and B. O. Roos, *Theor. Chim. Acta*, 1995, **90**, 87.
- 46 M. P. Fülcher and B. O. Roos, *Theor. Chim. Acta*, 1994, **87**, 403.
- 47 (a) Azulene: A. D. Hunter, E. E. Burnell and T. C. Wong, *J. Mol. Struct.*, 1978, **48**, 157; (b) Acenaphthylene: R. A. Wood, T. R. Welberry and A. D. Rae, *J. Chem. Soc., Perkin Trans. 2*, 1985, 451; (c) Fluoranthene: A. C. Hazell, D. W. Jones and J. M. Sowden, *Acta Crystallogr. Sect. B*, 1977, **33**, 1516; (d) Dibenzofuran: O. Dideberg, L. Dupont and J. M. André, *Acta Crystallogr. Sect. B*, 1972, **28**, 1002; (e) Dibenzothiophene: J. Kao, D. Leister and M. Sito, *Tetrahedron Lett.*, 1985, **26**, 2403.
- 48 K. Andersson, M. P. Fülcher, G. Karlström, R. Lindh, P.-Å. Malmqvist, J. Olsen, B. O. Roos, A. J. Sadlej, M. R. A. Blomberg, P. E. M. Siegbahn, V. Kellö, J. Noga, M. Urgan and P.-O. Widmark, *MOLCAS Version 3*, Dept. of Theor. Chem., Chem. Center, Lund University, POB 124, S-221 00 Lund, Sweden, 1994.
- 49 J. H. D. Eland, *Int. J. Mass Spectrom. Ion Phys.*, 1969, **2**, 471.
- 50 (a) W. Goldacker, D. Schweitzer and H. Zimmerman, *Chem. Phys.*, 1979, **36**, 15; (b) D. Schweitzer and H. Zimmerman, *Z. Naturforsch., Teil A*, 1979, **34**, 1185; (c) C. von Borczyskowski, F. Seiff and D. Stehlik, *J. Phys. Chem.*, 1987, **91**, 327.
- 51 C. Parkanyi, *Heterocycles*, 1982, **19**, 1237.
- 52 M. Zander and G. Kirsch, *Z. Naturforsch., Teil A*, 1989, **44**, 205.
- 53 B. Ruscic, L. Kovac, L. Klasinc and H. Güsten, *Z. Naturforsch., Teil A*, 1978, **33**, 1006.
- 54 G. Buemi, F. Zuccarello and G. Romeo, *J. Mol. Struct., THEO-CHEM*, 1983, **105**, 375.
- 55 M. Zander, J. Jacob and M. L. Lee, *Z. Naturforsch., Teil A*, 1987, **42**, 735.
- 56 R. A. W. Johnstone and F. A. Mellon, *J. Chem. Soc., Faraday Trans. 2*, 1973, **69**, 1155.
- 57 W. G. Herkstroeter, *J. Am. Chem. Soc.*, 1975, **97**, 4161.
- 58 D. Klemp and B. Nickel, *Chem. Phys.*, 1983, **78**, 17.
- 59 (a) M. J. S. Dewar and S. D. Worley, *J. Chem. Phys.*, 1969, **50**, 654; (b) M. J. S. Dewar, E. Haselbach and S. D. Worley, *Proc. Roy. Soc. London A*, 1970, **315**, 431; (c) R. Boschi, E. Clar and W. Schmidt, *J. Chem. Soc.*, 1974, **60**, 4406; (d) J. H. D. Eland and C. J. Danby, *Z. Naturforsch., Teil A*, 1968, **23**, 355.
- 60 E. Heilbronner, T. Hoshi, T. J. L. von Rosenberg and K. Hafner, *Nouv. J. Chim.*, 1976, **1**, 105.
- 61 S. Scypinski and L. J. Love, *Anal. Chem.*, 1984, **56**, 322.
- 62 A. Samanta and R. W. Fessenden, *J. Phys. Chem.*, 1989, **93**, 5823.
- 63 B. Nickel, *Helv. Chim. Acta*, 1978, **61**, 198.
- 64 (a) F. Pragst, R. Ziebig and E. Boche, *J. Luminescence*, 1979, **21**, 21; (b) J. Bello and R. J. Hurtubise, *Appl. Spectrosc.*, 1986, **40**, 790.
- 65 R. A. Femia and L. J. C. Love, *Spectrochim. Acta A*, 1986, **42**, 1239.
- 66 C. P. Butts, L. Ebersson, M. P. Hartshorn, W. T. Robinson and B. R. Wood, *Acta Chem. Scand.*, 1996, **50**, 587.
- 67 M. Zupan, J. Iskra and S. Stavber, *Tetrahedron*, 1996, **52**, 11341.

Paper 6/06702F  
 Received 30th September 1996  
 Accepted 1st November 1996